Eur. Phys. J. B **11**, 207–215 (1999)

THE EUROPEAN PHYSICAL JOURNAL B

EDP Sciences

Density functional study of the ternary Si_2CN_4 and C_{Si}: Si_3N_4 compounds

B. Amadon and F. Finocchi[a]

Laboratoire de Physique des Solides[b], Bâtiment 510, Université Paris-Sud, 91405 Orsay Cedex, France

Received 22 December 1998

Abstract. The structural and electronic properties of the recently synthesized ternary crystal Si_2CN_4 are investigated by means of density functional calculations, in comparison with pure and C–defective β Si_3N_4. The theoretical equilibrium lattice parameters of Si_2CN_4 well agree with experimental results, and the optimized atomic positions refine those extracted from diffraction data, permitting a precise description of the atomic structure. According to our calculations, the enthalpy of the reaction of dissociation of crystalline Si_2CN_4 into silicon nitride, silicon carbide and molecular nitrogen is positive, suggesting that the novel compound should be relatively stable at normal conditions, consistently with the experimental observation. The analysis of C_{Si}:β Si_3N_4, at low defect concentrations, either for scattered defect distributions or neighboring C_{Si}, reveals the presence of many dilated bonds. The microscopic stress is mainly responsible for the lower stability of carbon defective silicon nitride with respect to Si_2CN_4.

PACS. 71.15.Nc Total energy and cohesive energy calculations – 81.05.Je Ceramics and refractories (including borides, carbides, hydrides, nitrides, oxides, and silicides) – 61.72.Ji Point defects (vacancies, interstitials, color centers, etc.) and defect clusters – 62.20.Dc Elasticity, elastic constants

1 Introduction

The search for new non–oxide ceramics has undergone a rapid development in the last decade, due to the technological relevance of these compounds. They can have remarkable mechanical properties, such as hardness and plasticity, and improved resistance to high temperatures. On one hand, progress has been made in the design of binary CN_x systems, aiming to obtain ultra–hard materials [1]. Stoichiometric crystalline carbonitride C_3N_4, although theoretically predicted [2], has been experimentally obtained as disordered or microcrystalline phases [3–5] whose physical nature is still debated.

On the other hand, much work has been made to synthesize new C–N based compounds through the inclusion of other chemical species, such as silicon, which may favor the formation of tetrahedral bonding inside the network, and improve the mechanical properties. Recently, nanocrystalline SiC/Si_3N_4 composites with high tenacity and plastic behavior have been synthesized [6]. Other groups [7] have studied Si–C–N based nanocomposites, formed by sintering of powders obtained through laser pyrolysis of organic precursors. They found that an enhanced resistance to recrystallization towards SiC and Si_3N_4 can be obtained within a certain range of composition [8]. Further experimental investigations [8,9] showed that at temperatures lower than that needed to obtain recrystallization ($\simeq$ 1500 °C), these composites are formed by nanocrystalline grains inside an amorphous matrix. In all these phases, experimental evidence of Si–C, Si–N and C–N bonding was found, their precise ratio depending on temperature and macroscopic composition [10]. The X-ray and neutron diffraction data obtained from these powders were recently interpreted by means of a structural model in which C substitutes either Si or N in the α or β phases of silicon nitride [11]. Then, the discovery of crystalline Si_2CN_4 [12,13] demonstrated that it is finally possible to conceive ordered (meta)stable ternary systems, and therefore open new perspectives in the synthesis of Si–C–N based ceramics.

In comparison with these experimental improvements, theory has little advanced on the properties of ternary Si–C–N compounds. Preliminary results of density functional calculations are reported in reference [13], but they are still scarce and focus essentially on the properties of carbodiimide groups in various molecules and solids. Wang and coworkers [14] studied the structural properties of the β phase of hypothetical $Si_{3-x}C_xN_4$ in search of superhard materials, but nothing was said on the thermodynamical stability and the electronic properties of these compounds. Moreover, the success of the structural model for amorphous Si–N–C powders proposed in reference [11] calls for a more fundamental description of carbon defects in the silicon nitride network.

[a] e-mail: fabio@lps.u-psud.fr
[b] UMR CNRS 8502

In this paper, we present a theoretical investigation, based on density functional theory, of the structural and electronic properties of the crystalline compound Si_2CN_4 recently synthesized, and compare it with the inclusion of substitutional C defects in the β phase of Si_3N_4 (*i.e.* C_{Si}:β–Si_3N_4). The paper is organised as follows: after a detailed description of the computational ingredients, we give an account of the atomic structures as obtained in our simulations, in which both the internal (atomic positions) and the external (volume, lattice parameters) degrees of freedom are consistently optimized (only the type of the cell is kept fixed). Our structural results for Si_2CN_4 well compare to those obtained from X–ray diffraction [12]. Its bandstructure is discussed in relation with the nature of the chemical bonds in the material, and compared to molecular species and crystals showing the same kind of bonding. The last section is devoted to the discussion of the energetics: the thermodynamic stability of Si_2CN_4 is compared to that of C_{Si}:β–Si_3N_4 and other compounds.

2 Computational details

The electronic structure is described within the Density Functional Theory (DFT), in the Local Density Approximation (LDA), by using the Ceperley–Alder correlation energy as parametrized by Perdew and Zunger [15]. When calculating atoms or molecules in a polarized state, the spin extension to LDA (LSDA) is used. The selfconsistent electronic density is calculated through the scheme proposed by Car and Parrinello [16]. Soft, norm–conserving pseudopotentials are used to describe the interaction between the ionic core and the valence electrons [17]. The Kohn–Sham orbitals are expanded in a plane–wave basis set, up to a kinetic energy cutoff $E_{\rm cut}$. Although a cutoff as large as 60 Ry is necessary to get total energies converged within few tens of meV when using our pseudopotentials, we show in the following that a smaller $E_{\rm cut} = 40$ Ry is sufficient for most purposes. Plane waves are especially efficient when studying defects and unknown structures, since a single parameter ($E_{\rm cut}$) determines the quality of the basis set, which stays constant when changing structural parameters or the number and the type of the atoms in the unit cell. Geometry optimization is therefore rather simple to be carried out, and the energetics of compounds showing different bonding properties can be computed easily. Extensive applications to bulk, surfaces and clusters show the reliability of this method [18,19].

In order to assess the capability of our numerical approach to predict the structural properties and the energetics of Si–C–N based compounds, we perform several tests on known molecules and crystals, and compare our results to experimental data and other calculations. Firstly, for N_2, C_2, SiC_2 molecules and the CN radical, we calculate interatomic distances, stretching frequencies and dissociation energies. Most of the results are summarized in Table 1. One can see that the computed interatomic distances generally agree well with experimental data, which is usually the case for LDA calculations [18]. For the stretching frequencies discrepancies up to 5% are found, especially in the case of tightly bound molecules like N_2. This is a consequence of both the LDA and the choice of the pseudopotential. The use of a harder pseudopotential for nitrogen [20] would give frequencies closer to experiments and bond energies overestimated by about 15% ($d_{\rm eq} = 1.109$ Å, $\omega = 2325$ cm^{-1}, $D = 11.20$ eV). As far as the use of LDA or LSDA is concerned, the expected discrepancies for interatomic distances and frequencies range from 0% to 2%, depending on the specific system, and dissociation energies are generally overestimated from 10% to 20% [18]. One can also see from Table 1 that the use of either $E_{\rm cut} = 40$ Ry or $E_{\rm cut} = 60$ Ry does not modify the results appreciably. Regarding the SiC_2 molecule, we check that our method well compares to more refined quantum chemical calculations [21]. The C_{2v} configuration is found to be more stable of the C_∞ one by 0.19 eV. The computed interatomic distances are: 1.25 Å (C–C, C_{2v}), 1.27 Å (C–C, C_∞), 1.83 Å (Si–C, C_{2v}), 1.69 Å (Si–C, C_∞). We also compute the frequencies of the a_1 stretching modes (1819 cm^{-1} and 886 cm^{-1}), in good agreement with previous calculations and experiments.

Table 1. Calculated and experimental interatomic distances d, frequencies ω, and bond dissociation energy D of some diatomic molecules in their fundamental state ($^1\Sigma_g^+$ for N_2, $^3\Pi_u$ for C_2 and $^2\Sigma^+$ for CN). The values are computed either by using $E_{\rm cut} = 40$ Ry (†) or $E_{\rm cut} = 60$ Ry (‡). Other DFT results obtained by Chong [24] are also shown for comparison.

		N_2	C_2	CN·
d (Å)	Ref. [24]	1.095		1.166
	this work †	1.109	1.30	1.177
	this work ‡	1.101	1.31	1.175
	exp. (Ref. [22])	1.094	1.312	1.172
ω (cm^{-1})	Ref. [24]	2396		2137
	this work †	2230	1640	2060
	this work ‡	2210	1654	2035
	exp. (Ref. [22])	2360	1641	2069
D (eV)	Ref. [24]	11.38		9.33
	this work †	10.52	7.48	9.07
	this work ‡	10.59	7.51	9.09
	exp. (Ref. [23])	9.81	6.29	7.98

Then, we calculate structural properties (equilibrium lattice parameters, bulk modulus B and cohesive energy $E^{(\rm coh)}$) of O_h^7 Si, O_h^7 C, T_d^2 SiC and the β phase of Si_3N_4. For the latter, we use 2 special k points [25] in the irreducible part of the Brillouin zone for the integration of the charge density, and 10 special k points for Si, C, and SiC. Such a choice is sufficient to get converged total energies within few tens of meV/atom. Special care is used for β Si_3N_4, where both the internal (atomic coordinates in the unit cell) and the external (a, c) structural degrees of freedom have been optimized [26]. The total energy is calculated as a function of the latters by including a corrections due to the finite size of the basis set [27].

Table 2. Equilibrium lattice parameters a, c, bulk modulus B and cohesive energy per unit cell $E_{\rm coh}$ for the diamond phases of Si and C, for the zincblende phase of SiC and for the β phase (space group: $P6_3/m$) of Si_3N_4. Their unit cells contain 2, 2, 1, and 2 formula units, respectively. The theoretical values are computed by using $E_{\rm cut} = 40$ Ry. For β Si_3N_4, the structural properties computed by using the supercell approach are given in brackets, for the sake of comparison. The experimental data are taken from reference [23], apart from the cohesive energy of β Si_3N_4. It is obtained by adding the formation energies of crystalline silicon and molecular nitrogen to the enthalpy of formation of silicon nitride from the latters, as measured by O'Hare and coworkers (Ref. [31]).

		O_h^7 Si	O_h^7 C	T_d^2 SiC	β Si_3N_4
a (Å)	theory	5.39	3.55	4.325	7.60 (7.55)
	exp.	5.43	3.57	4.36	7.595
c (Å)	theory				2.90 (2.93)
	exp.				2.902
B (GPa)	theory	95	449	221	241 (235)
	exp.	99.2	443	230	256
$E_{\rm coh}$ (eV)	theory	10.74	17.52	14.75	97.0 (97.4)
	exp.	9.32	14.84	12.72	84.18

The computed structural properties, summarized in Table 2, well agree with experimental data.

For C_{Si}:β Si_3N_4, we use orthorhombic supercells containing 84 atoms, and sample the Brillouin zone with the Γ point only. The size of our supercell is estimated to be large enough to avoid spurious interactions between the periodic images for the small defect concentrations considered here, which correspond to either one or two C atoms per unit cell. The bias introduced by this choice is small, as it can be seen by comparing the structural properties of β Si_3N_4 computed within the supercell approach with those obtained through the more accurate sampling of the Brillouin zone (see Tab. 2). In order to reduce the numerical errors, in the following we compare the physical properties of C–defective silicon nitride with those of pure β Si_3N_4, both calculated in the supercell approach.

For orthorhombic Si_2CN_4, a $(2 \times 1 \times 2)$ supercell containing 112 atoms is used, with Γ point sampling. The total energy difference with respect to a calculation using a special k point in the irreducible part of the Brillouin Zone amounts to 0.08 eV/unit cell.

As far as the convergence with respect to the plane wave cutoff is concerned, the use of either $E_{\rm cut} = 40$ Ry or $E_{\rm cut} = 60$ Ry would modify the computed structural properties of 0.5% at most and it doesn't practically affect the atomic relaxations. We therefore adopt $E_{\rm cut} = 40$ Ry from now on, unless the contrary is explicitly said. In all our calculations, the lattice parameters defining our supercell are relaxed to their equilibrium values, so that the structural properties are computed at external zero pressure. The residual atomic forces at the end of the optimization runs never exceed 50 meV/Å.

3 Results and discussion

3.1 Atomic structure

In hexagonal β Si_3N_4 there are two inequivalent nitrogens, denoted as $N^{\rm I}$ and $N^{\rm II}$, which form a quasi–planar Si_3N configuration, almost parallel to the basal plane. The deviations from perfect planarity (which occurs when N and its three Si neighbors are on the same plane) can be estimated through the angle formed by the vector parallel to one of the Si–N bonds with the plane containing the other two, which does not exceed 5°. Our calculated Si–N bondlengths in β Si_3N_4 ($d_{\rm Si-N^{II}} = 1.72$ Å and $d_{\rm Si-N^{I}} = 1.735$ Å) well compare to the experimental values ($d_{\rm Si-N^{II}} = 1.730$ Å, $d_{\rm Si-N^{I}} = 1.704$, 1.728 and 1.767 Å) [29].

We study different configurations of C_{Si}:β Si_3N_4, where carbon substitutes silicon in the network, as a function of both the average concentration $n(C_{Si})$ (defined as the ratio of the C_{Si} atoms to the number of Si sites in the pure crystal) and the defect distribution. All the calculations are performed at zero external pressure, by letting the lattice parameters relax to their equilibrium values, since the lack of the optimization of the lattice parameters may bias the final values of the relaxed atomic positions. The reduction of the cell volume ranges from 1.5% at the lowest C_{Si} concentration ($n(C_{Si}) = \frac{1}{36}$), to $\simeq 2.5\%$ at $n(C_{Si}) = \frac{1}{18}$.

At $n(C_{Si}) = \frac{1}{36}$, C–N bondlengths are dilated (d_{C-N} ranges from 1.50 Å to 1.56 Å), with respect to β C_3N_4 (1.47 Å)[2]. This is mainly due to the geometrical constraints of the host crystal and results into a weakening of the C–N bond. The stress caused by the presence of C_{Si} extends over neighboring sites, as shown by the fact that the bondlengths between Si atoms and the nitrogens bound to carbon range from 1.74 Å to 1.78 Å. The deviations of the Si-N bondlengths from their equilibrium values in β Si_3N_4 appears to be slowly decreasing functions of the (Si, N) distance from the defect.

In principle, for supercells containing more than one C_{Si}, one has to consider distinct configurations, because of the inequivalence of nitrogen sites in β Si_3N_4. In practice, however, the physical properties of the defective crystal are by far more affected by the strong perturbation caused by the presence of C rather than by the particular choice of the C_{Si} site. Therefore, only two prototypical configurations having two C_{Si} per unit cell ($n(C_{Si}) = \frac{1}{18}$) are studied and compared. In the first one (1/18; A), the two carbons are bound to the same nitrogen, while in the second one (1/18; B) the two impurities are fourth neighbors (see Fig. 1). In order to distinguish among nitrogen sites having a different chemical environment, we denote with $N^{(j)}$ the nitrogens j-fold coordinated with carbon. As in the $n(C_{Si}) = \frac{1}{36}$ case, the C–N bonds turn out to be stretched. They range from 1.50 Å to 1.57 Å for the (1/18; B) configuration, and from 1.49 Å to 1.63 Å in the case of second neighbor carbons. While the (1/18; B) configuration show analogies with that at $n(C_{Si}) = \frac{1}{36}$, a non trivial relaxation of the C-N bonds occurs in the (1/18; A) configuration. In particular, the C-$N^{(2)}$ bondlengths

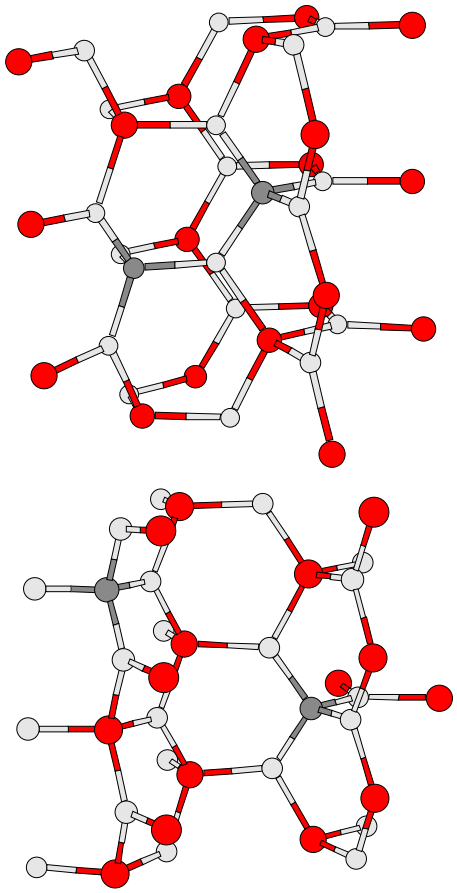

Fig. 1. Atomic structures of C_{Si}:βSi_3N_4, for the (1/18;A) (top) and (1/18;B) configurations (bottom). Si atoms are dark grey, C atoms grey and N atoms light grey. Only the atoms around the C_{Si} are drawn. One can note the distortion of the hexagonal cycles containing the C_{Si} defect.

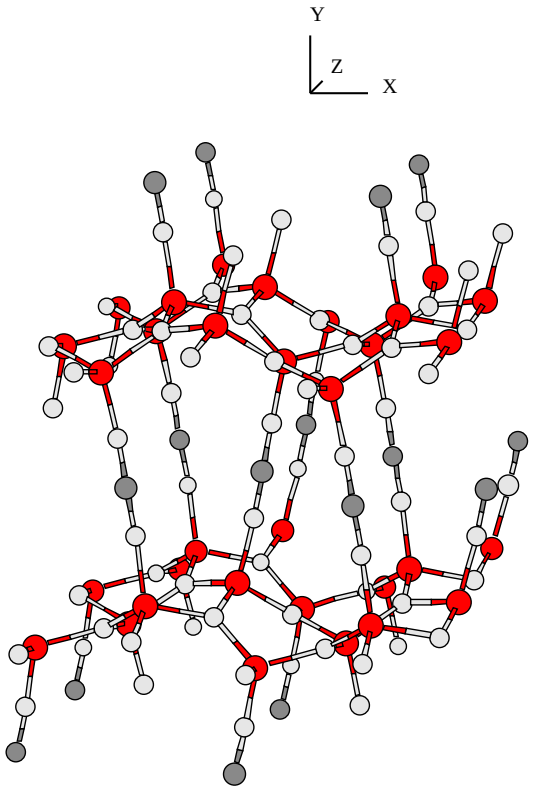

Fig. 2. Atomic structure of Si_2CN_4. The x, y and z directions, parallel to the axes a, b, c of the orthorhombic cell, respectively, are drawn. Si atoms are dark grey, C atoms grey and N atoms light grey.

Table 3. Calculated and experimental lattice parameters a, b, c, volume V and bulk modulus B of $Aaba2$ Si_2CN_4.

	a (Å)	b (Å)	c (Å)	V(Å^3)	B(GPa)
Theory	5.51	13.75	4.83	365.93	110
Exp. (Ref. [12])	5.44	13.58	4.81	355.34	

are greater than those for C-$N^{(1)}$. This is consistent with the larger stress affecting the $N^{(2)}$ atom, which is bound to two carbons, with respect to $N^{(1)}$ sites. As a result of the greater bond stretching, the (1/18; A) configuration is about 0.1 eV higher in energy than the (1/18; B) one. This picture also suggests an effective mechanism which might favor scattered distributions of C_{Si} in β Si_3N_4, at small C_{Si} concentrations.

In our simulations of Si_2CN_4, we started from the structure recently proposed by the analysis of X-ray diffraction data [12]. There are 28 atoms per unit cell, arranged in a structure with point group $Aaba2$. It can be viewed as a sequence of layers of distorted SiN_4 tetrahedra linked through N-C-N carbodiimide groups (see Fig. 2). There are no C-Si bonds. The presence of carbodiimide groups distinguishes Si_2CN_4 from other hypothetical compounds with the same stoichiometry, which may be obtained by replacing Si with C in silicon nitride.

The computed equilibrium lattice parameters of orthorhombic Si_2CN_4 well agree with experimental measurements (see Tab. 3). Si–N bonds for N within the Si–N rings give rise to a narrow distribution. Their bondlengths range from 1.71 Å to 1.72 Å, and are very similar to those found in β Si_3N_4. The bondlength between Si and the apical N (bound to C) is smaller (1.68 Å). Interestingly, also our calculated bondlength between carbon and nitrogen in Si_2CN_4 (1.21 Å) is smaller than the C=N double bondlength in other organic crystals [23]. A recent DFT calculation on $(NH_2)_3$Si-N=C=N-Si$(NH_2)_3$ [13] found 1.216 Å for the C=N bondlength, in close agreement with the present study. All these values are consistent with the remarkable strength of carbodiimide groups, and with the reinforced bonds between the latters and the Si–N distorted planes.

The shortest Si–N rings in Si_2CN_4 are sixfold and the deviation of Si_3N groups from perfect planarity is slightly more pronounced than in β Si_3N_4. The mean angle between a Si–N bond and the plane containing the two others bonds is equal to about 7°. Nevertheless, the bond angles in the two crystals are remarkably similar: in Si_2CN_4 we find that the distribution of θ_{N-Si-N} is centered around 110°, and $\theta_{Si-N-Si}$ around 119°. The angle θ_{Si-N-C}

on the apical nitrogen is equal to 167°, and the carbodiimide group is almost linear ($\theta_{\mathrm{N-C-N}} = 176°$). These results are in good agreement with those quoted in reference [13] for other molecules containing carbodiimide groups, apart from the small value (4°) of the dihedral angle between the (Si-N=C) and (C=N-Si) planes, which contrasts with its value found in those molecules ($\simeq 90°$).

The presence of carbodiimide groups deeply affects the elastic properties. On one hand, the bulk modulus of Si_2CN_4 (110 GPa) is strongly reduced with respect to pure and C–defective β Si_3N_4. On the other hand, the marked anisotropy of the former is shown by the large differences found among the elastic constants (Tab. 4), which can vary by a factor 10, depending on the direction of the virtual deformation (either parallel or normal to the carbodiimide groups). A more detailed discussion of the calculation of the bulk modulus from the computed elastic constants is given in the Appendix.

Table 4. Computed elastic constants (GPa) of *Aaba*2 Si_2CN_4. The error bar is 10 GPa.

c_{11}	c_{22}	c_{33}	c_{12}	c_{13}	c_{23}
210	440	180	60	25	140

3.2 Electronic structure

The bonding properties in Si_2CN_4 and in C_{Si}:β Si_3N_4 can be better analyzed by looking at the valence electronic charge density along both the Si-N and the C-N bonds, showed in Figure 3 for the case of pure β Si_3N_4 and β C_3N_4, computed at the equilibrium lattice parameters. The Si-N bond shows a marked ionic character, while along the C-N bond one can see an enhancement of the electronic density, consistent with a dominant covalent contribution. Our density profiles well agree with those previously calculated by Liu and Cohen [2]. We also note that no remarkable differences exist between the density profiles corresponding either to Si-N^{I} or to Si-N^{II} type of bonds, coherently with the fact that the Si-N^{I} and Si-N^{II} bondlengths are very similar (1.735 Å and 1.72 Å respectively). The same argument applies to C-N^{I} and C-N^{II}, too. In all these bonds the nitrogen shows a nearly sp^2-like hybridization with a variable degree of ionicity.

In Si_2CN_4, at variance, the valence charge density profile corresponding to the bond between the apical N and Si shows a slight accumulation of charge in the bond region on the nitrogen side, which results into a slightly more ionic Si-N bond compared to the Si-N bond within the sixfold rings. Consistently with the reduced coordination number, the bondlength between Si and the apical N is reduced (1.68 Å instead of 1.72 Å) and the cohesion between the Si-N rings and the carbodiimide groups is reinforced.

As discussed in the previous section, C-N bonds in C_{Si}: β Si_3N_4 are longer than in β C_3N_4, and indeed weakened.

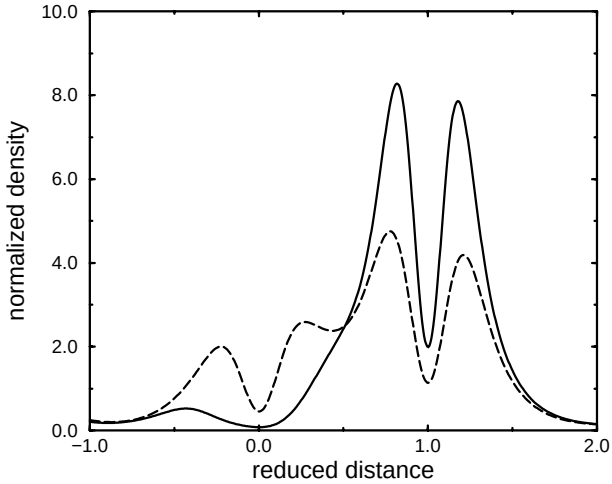

Fig. 3. Valence electronic charge density along the Si-N bond in β Si_3N_4 (full line) and the C-N bond in β C_3N_4 (dashed line). Reduced distances are used, so that the Si (C) atom is placed at 0 and the nitrogen atom at 1. The density profiles are in units of the average electronic density for the corresponding crystal.

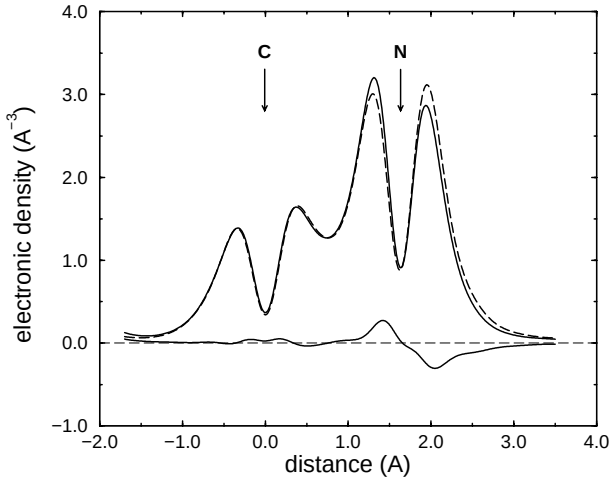

Fig. 4. Valence electronic charge density along the C-N bond in C_{Si}: β Si_3N_4 (dashed line) and the C-N bond in dilated β C_3N_4 (full line). The C-N bondlenghts are the same in the two cases, and the atomic sites are indicated by arrows. For the sake of clarity, also the *difference* between the two density profiles is plotted.

The first reason of such a dilatation lies in the geometrical constraints to which a carbon atom is subjected in the host Si_3N_4 lattice. It is also interesting to compare the charge density profiles along the C-N bond in C_{Si}: β Si_3N_4 and in β C_3N_4, to investigate possible changes in the electronic distribution. In order to point out the role of the host lattice in C defective silicon nitride, we compare in Figure 4 the density distribution along a C–N bond in C_{Si}: β Si_3N_4 with that of a isometric C–N bond in an hypothetically dilated C_3N_4. The main difference is seen around the nitrogen site: in pure C_3N_4 (both at the theoretical lattice parameter and dilated) the maximum occurs

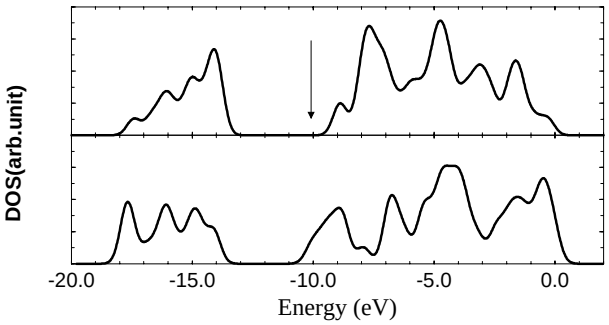

Fig. 5. Electronic density of states (DOS) of β Si_3N_4 (top panel) and Si_2CN_4 (bottom panel). The DOS are normalized so that their two integrals are the same. The arrow indicates the energy position of the deep C_{Si} state in C_{Si}: β Si_3N_4 at $n(C_{Si}) = \frac{1}{36}$.

on the bonding side, at variance with the electronic distribution in C_{Si}: β Si_3N_4. To recover the latter from that of dilated C_3N_4, one has to consider a polarization component on nitrogen, due to the neighboring Si cations, which decreases the C–N σ bonding contribution slightly.

The electronic density of valence states (DOS) of Si_2CN_4 is drawn in Figure 5, in comparison with that of β Si_3N_4. The DOS have been calculated for the two crystals by using the special points in the Brillouin zones, and then adding a $\simeq 0.5$ eV Gaussian broadening. A inner gap of $\simeq 4$ eV between two complex structures (the first one is comprised between -18 and -14 eV below the bottom of the valence band, the second one starts at -10 eV) is found. Three kinds of states contribute to the first structure: σ combinations with strong bonding character in carbodiimide groups (either $sp_N\, s_C\, sp_N$ at low energies, or $sp_N\, p_C\, sp_N$) and s orbitals of nitrogens in the SiN layers.

The second structure is rather complex, since it comes from bonding hybrids between N and C, on one side, and N and Si, on the other side, plus non-bonding nitrogen states at high energies. As far as the states mainly localized on the carbodiimide groups are concerned, in the range (-10 eV,-6 eV) we find σ molecular orbitals built from sp hybrids of nitrogens with evident bonding character with respect to the apical silicons, and only weak bonding character with carbon. At higher energies ($\simeq -5$ eV), we find π molecular orbitals on the carbodiimides. In this broad energy range (-10 eV, -3 eV), there are other relevant contributions, coming from p nitrogen states hybridized with Si, contributing to the Si-N bonds in the SiN layers. The upper part of the valence band, corresponding to the rightmost peak in Figure 5, comes essentially from non bonding p_N states.

The minimal gap between the valence and the conduction bands of Si_2CN_4 is found at the Γ point of the Brillouin zone. Its value, computed as the difference between the LDA eigenvalues, is equal to 4.3 eV. As it is generally underestimated [32], this value should rather be considered as a lower bound for one–particle excitations. It is therefore fully consistent with the experimental fact that pure Si_2CN_4 is found to be colorless [12]. The direct gaps computed at other points of the Brillouin zone can be up to 20% larger, as a consequence of the moderate dispersion. At the Γ point, the highest (lowest) state in the valence (conduction) band, that is, the HOMO (LUMO), is a π combination of non bonding (antibonding) N=C=N orbitals. States with non bonding (antibonding) character localized at the SiN layers appear at slightly lower (higher) energies with respect to the HOMO (LUMO). The characters of the HOMO and LUMO can be understood on the basis of a simple tight-binding model for a linear carbodiimide group whose dangling bonds are saturated by hydrogen. This comparison makes sense, since in Si_2CN_4 the carbodiimide group is almost linear and the dihedral angle between the Si-N=C and C=N-Si planes is very small (see Sect. 3.1).

3.3 Energetics

It would be of interest to know whether crystalline Si_2CN_4 is a thermodynamically stable phase or simply a metastable configuration in the ternary Si–C–N diagram. In the following we calculate the enthalpies of a few reactions, for which both crystalline Si_2CN_4 and defective C_{Si}:Si_3N_4 decompose into a mixture of simpler binary and elemental compounds. Among a variety of reactions, we choose the following two:

$$Si_{3-x}C_xN_{4\,(c)} \rightleftharpoons x SiC_{(c)} + (1-\frac{2}{3}x)Si_3N_{4\,(c)} + \frac{4}{3}x N_{2\,(gas)} \quad (1)$$

$$Si_{3-x}C_xN_{4\,(c)} \rightleftharpoons x C_{(c)} + (1-\frac{1}{3}x)Si_3N_{4\,(c)} + \frac{2}{3}x N_{2\,(gas)} \quad (2)$$

$x = 1$ corresponds to $Aaba2$ Si_2CN_4, and x =1/12 and 1/6 correspond to the two defect concentrations in C_{Si}:β Si_3N_4 ($n(C_{Si}) = \frac{1}{36}$ and $\frac{1}{18}$ respectively). The crystalline phases denoted with (c) are: $Aaba2$ for Si_2CN_4; β for pure and C–defective Si_3N_4; T_d^2 for SiC; diamond for C.

Reaction (1) is relevant, since the experiments show that the decomposition of several Si–C–N compounds, both in crystalline, nanocrystalline and amorphous phases, results in silicon carbide and silicon nitride, plus molecular nitrogen [8,12]. On the other hand, a reaction path analogous to that depicted in reaction (2), has been recently obtained for C poor Si–C–N nanopowders, which release carbon and approach the Si_3N_4 stochiometry as a function of the increasing temperature [11]. Moreover, the final products of reaction (2) are more stable than those considered in reaction (1) at normal conditions, according to experimental data [23,31]. Therefore, the two reactions written above are guidelines to a first understanding of the energetics of ternary Si–C–N compounds.

By means of our DFT calculations, we focus on the effect of the inclusion of carbon on the stability of the reactants ($Aaba2$ Si_2CN_4 or C_{Si}:Si_3N_4). In order to discuss this issue, we collect in Table 5 the computed enthalpies per C atom ($\Delta_r H/x$) of the reactions (1) and (2). One can see that $Aaba2$ Si_2CN_4 is stable against its decomposition into SiC, Si_3N_4 and N_2, which is the reaction

Table 5. Enthalpies of reaction normalized to x for the dissociation of $Si_{3-x}C_xN_4$ either in $xSiC + (1-\frac{2x}{3})Si_3N_4 + \frac{4x}{3}N_2$ (reaction (1)) or in $xC + (1-\frac{x}{3})Si_3N_4 + \frac{2x}{3}N_2$ (reaction (2)). Both *Aaba*2 Si_2CN_4 ($x = 1$) and the defective C_{Si}:β Si_3N_4 configurations at different C concentrations (1/36 or 1/18) are considered as reactants (see Sect. 3.1 and Fig. 1). $\Delta_r H$ is calculated at zero external pressure and absolute temperature. Zero–point effects are not included. In the third and fourth columns the calculated enthalpies are shown, and a lower bound (reaction (1), second column) and an upper bound (reaction (2), fifth column) for the enthalpies of the reactions are also given. See text for discussion.

	reaction (1)		reaction (2)	
$\Delta_r H$ / x (kJ/mol)	*l.b.*	calc.	calc.	*u.b.*
Si_2CN_4	+215	+285	−10	+20
C_{Si} Si_3N_4 (1/36)	+65	+135	−160	−130
C_{Si} Si_3N_4 (1/18; A)	+50	+120	−175	−145
C_{Si} Si_3N_4 (1/18; B)	+60	+130	−165	−135

observed experimentally at $T \simeq 1500$ °C, and more stable than C_{Si}:Si_3N_4 in both reactions. From the enthalpies of reaction of C–defective silicon nitride, the scattered defect distribution (B) at $n(C_{Si}) = \frac{1}{18}$ turns out to be slightly favored.

A question naturally arises, about the reliability of the computed enthalpies of reaction. In our calculations, we have two major sources of error, coming from the use of pseudopotentials and of the LDA. The LDA is known to give systematically too large binding energies (see Tab. 1, 2 and Ref. [18]), so that at first sight our results may be questionable. Nevertheless, when calculating *energy differences*, some of this error may be eliminated. This compensation is especially effective when reactions in which the nature of bonding does not vary too much are considered. For instance, the computed enthalpy of reaction Si + C → SiC (−60 kJ/mol) agrees very well with the experimental value of −62 kJ/mol, which can be easily calculated from Table 2. It is therefore worth estimating upper and lower bounds for the computed enthalpies of reactions (1, 2).

Thus, we introduce the quantity ΔD(A−B), defined as the difference between our computed $D_{\rm th}$(A−B) and the experimental $D_{\rm exp}$(A−B) A-B bondstrengths in a given compound. Let's consider, for instance, the reaction (1) for C_{Si}:β Si_3N_4, where 4 Si-C + 4/3 N≡N bonds are created, and 4 C-N + 4 Si-N bonds destroyed. The difference between the computed and the experimental enthalpy of reaction per C atom (*i.e.* our error ΔE) can thus be rewritten as

$$\Delta E = 4\,\Delta D(\mathrm{C{-}N}) + 4\,\Delta D(\mathrm{Si{-}N}) - 4\,\Delta D(\mathrm{Si{-}C}) - \frac{4}{3}\,\Delta D(\mathrm{N{\equiv}N}).$$

Since experimental determinations of the C-N bondstrength ($D_{\rm exp}$(C-N)= 298 kJ/mol [23]) are available only for organic molecules, we approximate $\Delta D(\mathrm{C{-}N}) \simeq [D_{\rm th}(\mathrm{C{\doteq}N})/D_{\rm exp}(\mathrm{C{\doteq}N}) - 1]\, D_{\rm exp}(\mathrm{C{-}N})$, where the first term in brackets is the ratio between the computed and experimental dissociation energies of the CN radical (see Tab. 1). The estimate of ΔD(C-N) is expected to be reliable, since the LDA yields a relative overbinding which is roughly constant for various bonds. By using the numerical values in Tables 1 and 2, we see that our calculation overestimates the stability of the reactants in reaction (1) by about 70 kJ/mol. This value is used in Table 5 to give a *lower* bound for the stability of the reactants. By taking into account the occurrence of stretched Si-N and C-N bonds in C_{Si}:Si_3N_4, one would get a slightly smaller error ΔE.

The case of reaction (2) is unlike. By proceeding as above, the difference between the computed and the experimental enthalpies for this reaction amounts to about −30 kJ/mol, which means that the stability of products is overestimated by our calculation. An *upper* bound can thus be given for $\Delta_r H$ in reaction (2).

Our results suggest that at zero pressure and temperature Si_2CN_4 is stable against decomposition into silicon carbide and silicon nitride. On the other hand, when T increases, the entropic contribution to the Gibbs free energy $G = H + TS$, may stabilise the products of reaction (1). An estimate of $T\,\Delta_r S$ between the products of the two reactions can be made by taking into account only the entropy of 2/3 mol of N_2 in the gas phase, which gives, at $T \simeq 1500$ °C, $T\,\Delta_r S$ of the same order of $\Delta_r H$. These considerations might explain the observed recrystallization of ternary Si–C–N compounds in SiC and Si_3N_4, plus molecular nitrogen, at $T \simeq 1500$ °C [8,11,12], although the enthalpy difference between the products of reactions (1) and (2) is larger than 200 kJ/mol, favoring the occurrence of reaction (2) at low temperatures.

The entropic contribution should likely favor the continuous loss of nitrogen, above a temperature which roughly corresponds to 1000 °C according to the experimental data. The resulting amorphous compound, whose Si/N ratio is larger than 2, might be thermodynamically less stable than the crystalline phases of silicon carbide plus silicon nitride. A further temperature increase could thus be sufficient to induce the irreversible transformation into polycrystalline SiC/Si_3N_4.

C_{Si}:β Si_3N_4 turns out to be much less stable than Si_2CN_4. By looking at the reaction $Si_{3-x}C_xN_4 \rightarrow \frac{x}{3}C_3N_4 + (1-\frac{x}{3})Si_3N_4$, one can note that both the number and the type of bonds stay constant when considering C defective silicon nitride as reactant. For this reaction, $\Delta_r H/x$ is $\simeq -160$ kJ/mol, consistently with Si-N and C-N bonds more stretched, and indeed weaker, in C_{Si}:β Si_3N_4 than in the separated binary compounds. This also suggests that other ternary compounds obtained through replacement of Si or N with C atoms in crystalline silicon nitride might be thermodynamically not very stable.

4 Conclusions

Our density functional calculations show that the recently synthesized Si_2CN_4 is stable, at zero pressure and temperature, with respect to the decomposition into silicon

$$B_0 = \frac{(c_{11}c_{22}c_{33} + 2c_{12}c_{13}c_{23} - c_{11}c_{23}^2 - c_{22}c_{13}^2 - c_{33}c_{12}^2)}{(c_{11}c_{22} + c_{11}c_{33} + c_{22}c_{33} + -2c_{11}c_{23} - 2c_{22}c_{13} - 2c_{33}c_{12} + 2c_{12}c_{13} + 2c_{13}c_{23} + 2c_{12}c_{23} - c_{12}^2 - c_{13}^2 - c_{23}^2)}. \quad \text{(A.2)}$$

carbide, silicon nitride and molecular nitrogen. A reaction enthalpy close to zero is obtained when considering diamond, nitrogen and silicon nitride as products, but the experimental relevance of this reaction is uncertain, since the dissociation of Si_2CN_4 into binary or elemental compound generally follows the other path. Moreover, because of the presence of carbodiimide groups, which are tightly bound to the SiN distorted layers in Si_2CN_4, the activation barrier to be overpassed would possibly be rather large. Si_2CN_4 is a wide gap compound, like β Si_3N_4, but much softer than the latter, as shown by the computed elastic constants.

On the other hand, C_{Si}:β Si_3N_4 turns out to be less stable. The inclusion of carbon in the silicon nitride network causes a long range microscopic stress. As a result, many bonds are stretched and the cohesive energy is lowered. Our calculations suggest also that, at low C_{Si} concentrations, clustered distributions of defects would not be energetically favored.

It is a pleasure to thank Claudine Noguera for fruitful discussions. We acknowledge support from the CNRS through GDR 1168. The computational resources were provided by CEA under project No. P52 and IDRIS/CNRS under project No. 980864. This paper is dedicated to the memory of Christiane Sénémaud, whose experimental work and warm encouragement motivated us to start the present study.

Note added in proof

In a recent paper (Phys. Rev. B **60**, 3126 (1999)) Kroll, Riedel and Hoffman studied the ternary SiC_2N_4 and Si_2CN_4 compounds theoretically. Their results for the latter well compare to ours, apart from a slight underestimate of $\Delta_r H$ for $Aba2$ Si_2CN_4 in reactions (1) and (2).

At variance with the present work, Kroll and coworkers evaluated $\Delta_r H$ by using different approximations of the exchange-correlation functional for the extended and the molecular phases. This might be the reason of the discrepancies with our results.

Appendix: Calculation of bulk modulus

As a general rule, an external hydrostatic pressure induces an anisotropic volume relaxation in non cubic crystals. In this appendix, we give the expression for the bulk modulus B_0 as a function of the elastic constants c_{ij} of orthorhombic crystals, by taking into account the anisotropic volume relaxations.

The elastic energy U, expressed as a function of the cell deformations, is minimized subject to the condition that V be held constant by using a Lagrange multiplier. Thus, the analytical expression of the elastic energy as a function of the volume variations $(V - V_0)$ is obtained:

$$U = U_0 + B_0 \frac{(V - V_0)^2}{2V_0} + o\,(V - V_0)^3, \quad \text{(A.1)}$$

where the bulk modulus at equilibrium (B_0) is given by:

see equation (A.2) above.

The quantities with the 0 subscript are equilibrium values. By keeping the equilibrium cell shape constant as a function of the applied pressure, one would obtain another expression, say $\tilde{B}_0$, for the bulk modulus:

$$\tilde{B}_0 = \frac{c_{11} + c_{22} + c_{33} + 2c_{12} + 2c_{13} + 2c_{23}}{9}. \quad \text{(A.3)}$$

Whenever $\tilde{B}_0$ is computed at the minimum (a_0, b_0, c_0), it cannot be smaller than B_0; their difference is slight whenever $c_{11} \simeq c_{22} \simeq c_{33}$ and $c_{12} \simeq c_{23} \simeq c_{13}$, but it may be appreciable for very anisotropic crystals. For instance, in Si_2CN_4 we find B_0=110 GPa and $\tilde{B}_0$=140 GPa (see Tab. 4). We note that the use of the elastic energy as written in equation (A.1) implies that the internal degrees of freedom (*i.e.* the atomic positions) are optimized whatever the cell deformation.

References

1. See, *e.g.*, J.V. Badding, Adv. Mater. **9**, 877 (1997) and references therein.
2. A.Y. Liu, M.L. Cohen, Phys. Rev. B **41**, 10727 (1990).
3. A.R. Merchant *et al.*, J. Appl. Phys. **79**, 6914 (1996).
4. K.M. Yu *et al.*, Phys. Rev. B **49**, 5034 (1994).
5. J. Martin–Gill *et al.*, J. Appl. Phys. **81**, 2555 (1997).
6. K. Niihara, J. Mater. Sci. Lett. **10**, 112 (1990).
7. N. Herlin, M. Luce, E. Musset, M. Cauchetier, J. Europ. Ceram. Soc. **13**, 285 (1994).
8. J. Dixmier, R. Bellissent, D. Balhoul, P. Goursat, J. Europ. Ceram. Soc. **13**, 293 (1994); J. Dixmier *et al.*, Fourth Eur. Ceram. **1**, 233 (1995).
9. F. Ténégal, A.-M. Flank, N. Herlin, Phys. Rev. B **54**, 12029 (1996).
10. M. Driss-Kodja *et al.*, Phys. Rev. B **53**, 4287 (1996).
11. F. Ténégal *et al.*, Phil. Mag. A **78**, 803 (1998).
12. R. Riedel *et al.*, Angew. Chem. **36**, 603 (1997).
13. R. Riedel *et al.*, Chem. Mater. **10**, 2964 (1998).
14. C.-Z. Wang, E.-G. Wang, Q. Dai, J. Appl. Phys. **83**, 1975 (1998).
15. D.M. Ceperley, B.J. Alder, Phys. Rev. Lett. **45**, 566 (1980); J.P. Perdew, A. Zunger, Phys. Rev. B **23**, 5048 (1981).
16. R. Car, M. Parrinello, Phys. Rev. Lett. **55**, 2471 (1985).

17. N. Troullier, J.L. Martins, Phys. Rev. B **43**, 1993 (1991). s and p components are retained for both C and N, while the inclusion of d pseudopotential has been proven to be necessary for Si. The cutoff radii in atomic units are chosen as follows: 1.50 for $2s$ and $2p$ states of C; 1.40 ($2s$, N) and 1.60 ($2p$, N); 1.50 ($3s$, Si), 1.75 ($3p$, Si) and 2.20 ($3d$, Si).
18. See, *e.g.*, O. Gunnarsson, R.O. Jones, Rev. Mod. Phys. **61**, 689 (1989).
19. F. Finocchi, C. Noguera, Phys. Rev. B **53**, 4987 (1996); F. Finocchi, J. Goniakowski, C. Noguera, Phys. Rev. B **59**, 5178 (1999).
20. This pseudopotential is generated by using cutoff radii of 0.75 a.u. for both the s and p channels. Due to the high energy cutoff ($\simeq$ 160 Ry) necessary to converge the total energy of the nitrogen dimer, it cannot in practice be used when treating large systems.
21. I.B. Nielsen, W.D. Allen, A.G. Császár, H.F. Schaefer III, J. Chem. Phys. **107**, 1195 (1997).
22. G. Herzberg, *Molecular spectra and molecular structure*, 2nd edn. (Van Nostrand, New York, 1966).
23. *Handbook of chemistry and physics*, edited by D.R. Lide (CRC Press, 1992).
24. D.P. Chong, Chem. Phys. Lett. **220**, 102 (1994).
25. The two special k points have coordinates (in units of $2\pi/a$): $k_1 = (\frac{1}{3}, \frac{1}{3\sqrt{3}}, \frac{3}{8}\frac{a}{c})$, $k_2 = (\frac{1}{3}, \frac{1}{3\sqrt{3}}, \frac{1}{8}\frac{a}{c})$. They are sufficient to annul the symmetrized combinations of plane waves up to the fourth coordination shell included. For the cubic structures, the ten special points are taken from Chadi, M.L. Cohen, Phys. Rev. B **8**, 5474 (1972).
26. Here we assume the $P6_3/m$ point group, as suggested by R.W.G. Wyckoff, in *Crystal structures* (Wiley, New York, 1964). Although $P6_3$ seems to be better consistent with recent X-ray diffraction data (Ref. [29]) the deviations of the atomic coordinates from the special positions $z/c = 0.25$ as found in our symmetry unrestricted supercell calculations are within the precision of the method.
27. G.M. Rignanese, Ph. Ghosez, J.-C. Charlier, J.-P. Michenaud, X. Gonze, Phys. Rev. B **52**, 8160 (1995).
28. F.D. Murnaghan, Proc. Nat. Acad.Sci. USA **50**, 697 (1944).
29. R. Grün, Acta Cryst. B **35**, 800 (1979).
30. H.M. Seip, Acta Chem. Scand. **15**, 1789 (1961).
31. P.A.G. O'Hare, I. Tomaszkiewicz, H.J. Seifert, J. Mater. Res. **12**, 3203 (1997).
32. R.W. Godby, M. Schlüter, L.J. Sham, Phys. Rev. B **37**, 10159 (1988).